SITE ATMOSPHERIC CHARACTERIZATION

Marc Sarazin
European Southern Observatory

Abstract

As adaptive optics techniques turn into integrated self-optimized systems, a new infrastructure is proposed to answer the need of an independent routine monitoring of the spatiotemporal behavior of the optical turbulence above large ground-based telescopes.

1.- INTRODUCTION

The past decade has seen the development of new devices to reliably monitor atmospheric seeing and a few observatories are now routinely proposing to the observers new services including online visualization of the site seeing in addition to standard meteorological parameters. The differential image motion (DIMM) method is also widely used for ongoing site surveys in China, South-Africa, Namibia and even Antartica.

As adaptive optics techniques come out of the prototype phase and turn into integrated systems, designers are urging for independent routine monitoring of additional atmospheric parameters characterizing the spatiotemporal behavior of the optical turbulence above large ground-based telescopes. The ambitious goal is to obtain in real-time the velocity, direction and altitude of the fluctuations of the index of refraction and their spatial coherence as well.

The aim of this paper is to review the quantities involved and to describe some of the experimental setups currently available to the community.

2.- THE PARAMETERS INVOLVED

Each thermally turbulent layer, characterized by its altitude, velocity, direction, outer scale and index of refraction structure coefficient, will affect the wavefront, creating phase and amplitude corrugations. The former to be later corrected by the adaptive optical element of the telescope or instrument.

For classical imaging, the effects of successive turbulent layers are purely additive in terms of index of refraction structure coefficient and give birth to the well known *seeing*, characterized at the telescope by the Fried parameter r_0 of the wavefront in the entrance pupil plane or the FWHM (Full Width at Half Maximum of a stellar image) in the focal plane.

The altitude of a given layer changes its apparent angular scale, as viewed from the telescope, and thus determines its contribution to the *isoplanatic angle*, defined as the maximum angular separation of two stellar objects producing identical wavefronts at the telescope entrance pupil. The isoplanatic angle is a major restriction to the selection of bright reference stars in the surrounding of a faint object observed with adaptive optics. The higher the turbulence occurs above the telescope, the smaller is the available portion of sky. A selection of a reference star outside the isoplanatic field decreases the correction efficiency by adding noise in the higher orders.

An Adaptive Optics system is mainly sensitive to the speed at which the phase of the wavefront moves over the pupil. The fact that not all layers move in the same direction creates a distinction between the boiling part of the short exposure wavefront corrugations and the frozen part. In other words, one defines for the set of turbulent layers a dispersion velocity and a mean characteristic velocity , the latter associated to a mean direction of motion, determines the *optimum response time* of the correction system.

Finally, the *outer scale of the wavefront*, a weighed combination of the geophysical outer scales in the set of layers will determine in particular the shape of the tilt power density spectrum after averaging by the pupil of the telescope [Sasiela 94], and decide whether tilt correction is necessary on large telescope systems.

Those tuning parameters vary in time by a large magnitude because the vertical distribution of thermal turbulence is rarely immutable. However few measurements are available, we show some of them in what follow.

3.- THE PARANAL SEEING CAMPAIGN (PARSCA)

This campaign was a first step towards a more ambitious goal in relation with emerging high resolution imaging techniques, ie: to measure more exotic parameters named speckle lifetime or isoplanatic angle and to point out, for future modeling, existing relationship with standard atmospheric parameters recorded daily all over the world by means of balloon borne meteorological radiosoundings.

It is agreed that Cerro Paranal emerges among the world outstanding sites with respect to cloudiness, precipitable water vapour content of the atmosphere and image quality, but little is known about the temporal behavior of the wavefront. This is precisely to gain insights about how high above the site the thermal turbulence travels and how fast it moves that the PARSCA campaign was organized as a collaboration between ESO and the Astrophysics Department of Nice University.

Over a duration of 14 nights in March 1992, 20 meteorological balloons with microthermal sensors were launched from the foot of Paranal to get them as close as possible to the summit during the initial phase of their ascent. A SCIDAR measuring turbulence via double stars with a 80 cm diameter collector mounted in a sea-container, was installed at the ESO base camp 300 m below the summit (this instrument is sensitive only to the atmospheric layers at more than 1km over ground). The SCIDAR measurements were repeated at the same period in 1993. As shown on Fig. 1, the $C_n^2(h)$ profiles obtained with either instruments are in rather good agreement below the tropopause, but the balloon profile is more pessimistic in the stratosphere. Although such discrepancies have little effect on the integrated seeing due to the small turbulence involved, they are more relevant in the estimates of isoplanatic angle and coherence time due to the altitude weighing functions which enter into the computation. The $C_n^2(h)$ at Paranal has been compared in Fig. 1 to a Hufnagel-Valley Boundary model, modified by [Olivier 94] to coincide with SCIDAR profiles obtained in 1987 above Mauna Kea. The Mauna Kea model and the Paranal balloon profiles are both arbitrarily normalized to yield the same optical seeing of 0.75 arcsec.

Similarly, wind profiles are presented on Fig. 2, comparing Mauna Kea and Paranal. The two sites have a very comparable high altitude environment, the broader peak at Mauna Kea could be an artifact due to the low vertical resolution of the Hilo soundings used to derive the model. An orographic wind regime is clearly present in the first 1000 m above paranal, again its absence in the Mauna Kea model could be due to the fact that the balloons were not launched from the site itself.

Finally, Fig. 3 shows results about the various parameters one can compute mixing the previous turbulence and wind profiles. The parameter definition is the same as used for similar measurements at La Palma ([Vernin 94]), where the even more limited set of results (5 nights) shows smaller isoplanatic angles and a similar, but more stable, temporal coherence.

The interest of flexibly scheduling telescope operation is highlighted by the PARSCA results, in particular the nights of March 12 and 14, showing a ten fold decrease of coherence time and isoplanatic angle after a change in meteorological conditions. This change is also visible in the value of the maximum wind speed; however, considering the whole set of flights, there is no

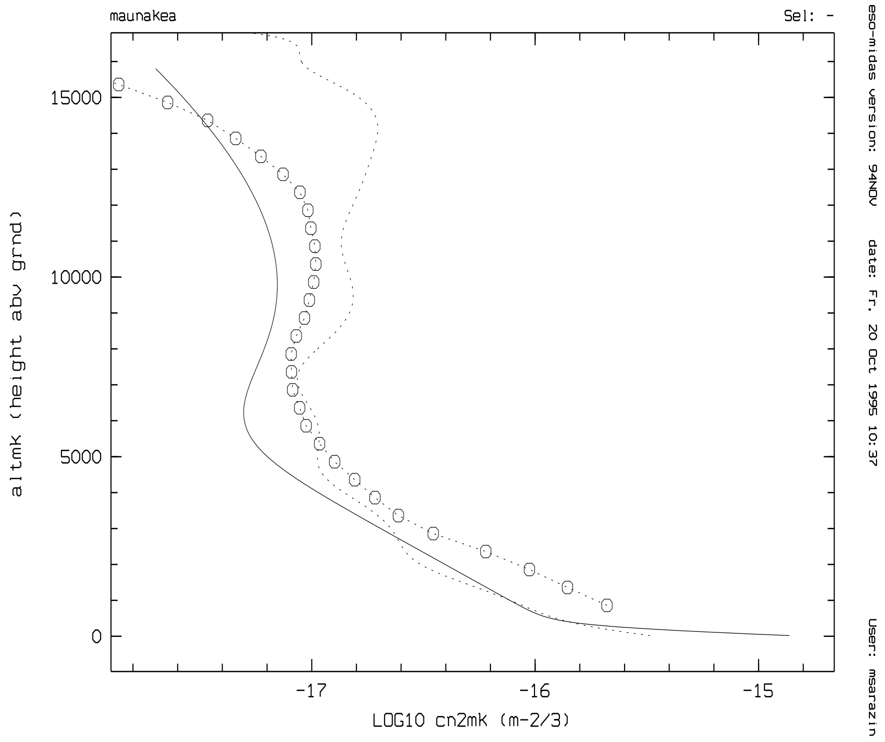

Figure 1: Results of the PARSCA campaign: comparison of turbulence profiles at Mauna Kea ([Olivier 94], modified Hufnagel-Valley, full line) and at Paranal with the SCIDAR (dots, 1993 campaign) and the balloons (dashed line, 1992 campaign).

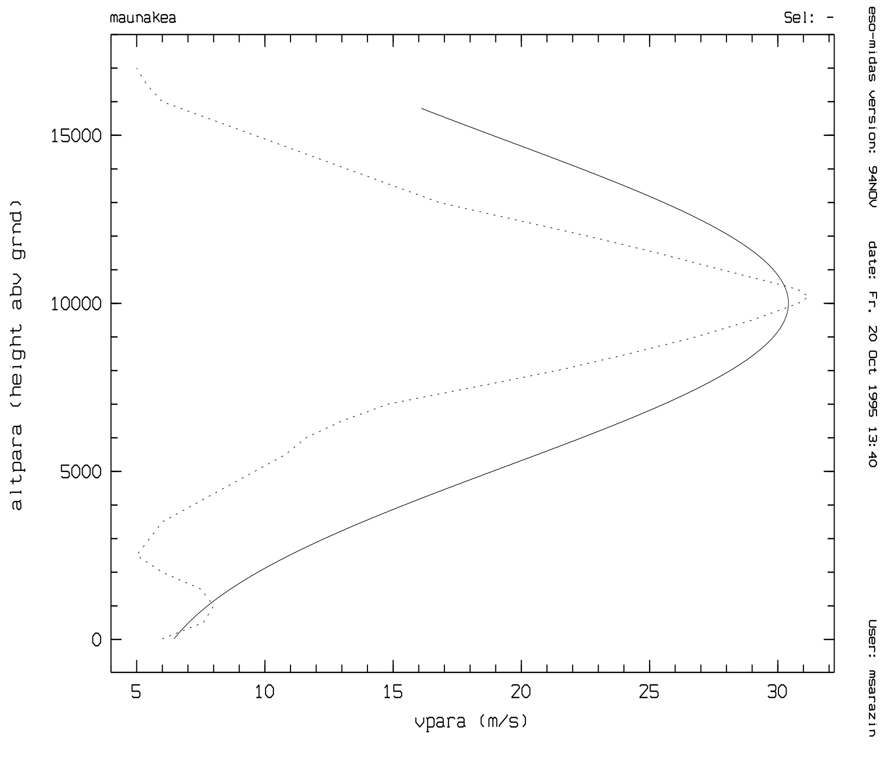

Figure 2: Results of the PARSCA campaign: Vertical wind profile at Paranal ([Fuchs 95], dashed line) compared to wind above Mauna Kea modeled from Hilo radiosoundings by [Olivier 94].

Flight (UT)	L0 (m)	R0 (cm)	ThAO (")	ThSI (")	TauAO (ms)	TauSI (ms)	Vmax (m/s)	V0 (m/s)	H2O (mm)
09/3/92 3h30	1.55	26.5	3.0	4.1					1.9
10/3/92 3h30	1.18	29.3	3.8	4.8					2.9
11/3/92 4h45	4.10	12.1	4.1	4.3	10.9	14.8	28	3.9	2.9
12/3/92 1h30	2.38	17.2	3.5	3.8	14.5	20.5	18	4.2	2.5
14/3/92 3h30	6.76	6.7	0.4	0.8	1.2	2.2	42	18.0	4.3
15/3/92 1h00	2.09	18.5	2.0	2.9	5.2	7.4	48	11.1	5.5
15/3/92 5h00	1.70	21.7	1.7	3.2	3.4	6.2	55	19.7	4.3
16/3/92 4h10	2.11	13.7	2.5	2.7	7.9	13.3	25	6.6	3.7
24/3/92 8h12	2.40	12.1	1.6	2.1	3.9	4.9	43	10.0	3.4
25/3/92 2h43	2.51	18.1	2.0	2.6	3.3	5.8	45	22.1	1.6
25/3/92 7h11	1.30	15.9	2.2	2.5	3.5	6.3	58	16.8	3.4
29/3/92 4h10	1.48	16.1	2.8	3.2	4.9	17.7	20	11.1	4.9
29/3/92 9h15	1.92	10.9	1.7	1.9	3.3	11.6	18	9.8	5.0

Meaning of parameters:
L0: outer scale of turbulence (using Coulman Vernin Model)
R0: Fried Parameter
ThAO: Isoplanatic angle for Adaptive Optics
ThSI: Isoplanatic angle for Interferometry
TauAO: Coherence time for Adaptive Optics
TauSI: Coherence Time for Interferometry
Vmax: Maximum wind velocity (in the troposphere)
V0: Average wavefront Velocity (frozen Atmosphere)
H2O: precipitable water vapour content

Figure 3: Results of the PARSCA campaign as processed by ([Fuchs 95]).

simple relation between maximum wind speed indicating jet stream proximity, and wavefront parameters.

A better understanding of the mechanisms triggering optical turbulence as in [Coulman 95] is still needed before one can use predictable meteorological variables for the prediction of astronomical observing conditions.

4.- SEEING PREDICTION: THE POINT-AHEAD MULTI-DIMM METHOD

4.1- The frozen turbulence hypothesis

To stay in agreement with the physical model proposed by [Coulman 95] the classical Taylor hypothesis of a 'frozen atmosphere' moving at the average velocity of the flow has to be restricted to individual layers inside which the spatial fluctuations of the potential temperature follow the inertial law of the Kolmogorov turbulence spectrum. The thickness of such layers is characterized by their outer scale of turbulence L_0 inside which the strength of the turbulence is given by a single structure coefficient. It is important to note that, in a stably stratified nocturnal atmosphere, the spatial scale of thermal turbulence can be much smaller than the scale of the largest dynamic vortices.

A few years ago, seeing and scintillation have been monitored simultaneously with identical instruments during several nights at two astronomical observatories in Chile: Las Campanas and La Silla, distant of 27 km in the direction of the prevailing wind. The results given in [Sarazin 92] show that the normalized temporal intercorrelation of the two seeing time series presents a well defined peak corresponding to a 50 minute delay of La Silla with regards to Las Campanas, thus an average wind velocity of 9 m/s at the turbulence height.

The good correlation of the signals showed that turbulence in the atmosphere conserves its features over long distances. These properties may be used for predicting, circa one hour in advance, observing conditions at modern ground based astronomical observatories as an input to a knowledge based telescope scheduler during flexible operation.

4.2 The Point-Ahead method: first results

Rather than having to monitor from different locations, we investigate the feasibility of seeing prediction by differential seeing measurements at high and low airmass (Fig.4) obtained from the same place. For this purpose, two DIMMs were operated side by side on a 5 m high tower.

The time series of Fig. 5 was recorded at La Silla, a site usually dominated by low altitude turbulence traveling southwards. The intercorrelation function (Fig. 6) shows a clear lead of the northern horizon signal with respect to the zenith seeing, with a broadening of the correlation peak. The wind velocity at ground level was between 2 and 3 m/s from the direction NNE. Assuming a uniform vertical profile for the wind velocity, the corresponding point-ahead distance is 3 km. For a 20 degrees elevation angle, the bulk of the turbulent would be at a maximum altitude of 1000 m above the site level.

The low value of the intercorrelation function at lag 0 indicates a low level of turbulence traveling in the transverse (West-East) direction. More extensive measurements will be realized at Paranal in the coming months: Paranal is mainly dominated by high altitude turbulence traveling eastwards. We could thus expect much larger lead times for a western horizon signal, more compatible with the VLT operational requirements.

CONCLUSION

The Astronomical Site Monitor of the VLT Observatory will provide on line meteorology and seeing informations to the observers, telescope operators and expert systems. An even more ambitious goal is to predict observing conditions one hour in advance.

It may be possible to conceive Adaptive Optics systems which periodically (eg.: ca. 5 min) optimize their operating parameters. If this is the case, it is necessary to design reliable instruments, attached to the observatory rather than to individual telescopes, capable of accurately depicting the current observing environment.

ACKNOWLEDGEMENTS

The success of the PARSCA Campaign was mainly due to the excellent team of the Astrophysics Department at Nice University: M. Azouit, A. Fuchs, J.F. Manigaut and J. Vernin.

We thank D. Bonaccini and A. Renzini for their initial suggestion of the point-ahead method, and J. Navarrete for setting up the experiment on such a short notice.

REFERENCES

[Coulman 95]: C.E. Coulman, J. Vernin and A. Fuchs; *Optical Seeing: mechanism of formation of thin turbulent laminae in the atmosphere*; Applied Optics, Vol. 34, No:24, August 1995.

[Fuchs 95] A. Fuchs, *Contribution à l'étude de l'apparition de la turbulence optique dans les couches minces. Concept du scidar généralisé*; PHD Thesis, April 1995, Univ. of Nice, Astrophysics Dept.

[Olivier 94] S.S. Olivier, D.T. Gavel; *Tip-tilt compensation for astronomical imaging*; J. Opt. Soc. Am. A, Vol. 11, No. 1, January 94, 368-378.

[Roddier 90]: F. Roddier et al.; *Seeing at Mauna Kea: a joint UH-UN-NOAO-CFHT study* ; SPIE, Vol. 1236-42, p485-492, Advanced Technology Optical Telescopes IV, Tucson, 1990.

[Sarazin 92]: M. Sarazin; *The use of the large spatial coherence of turbulence patterns for predicting observing conditions in astronomical observatories*; International Meeting for wave propagation in random media; Seattle Wa, Aug. 3-7, 1992; *and* Atmos. Oceanic Opt. **5**, 12, Dec. 1992 (translated from Russian).

[Sasiela 94]: R.J. Sasiela; *Electromagnetic Wave Propagation in turbulence, Evaluation and Application of Mellin transforms*; Springer Verlag, 1994.

[Vernin 94]: J. Vernin, C. Muñoz-Tuñón; *Optical Seeing at La Palma Observatory: II. Intensive Site Testing Campaign at the Nordic Optical Telescope*; Astron. Astrophys. 284, 311-318 (1994).

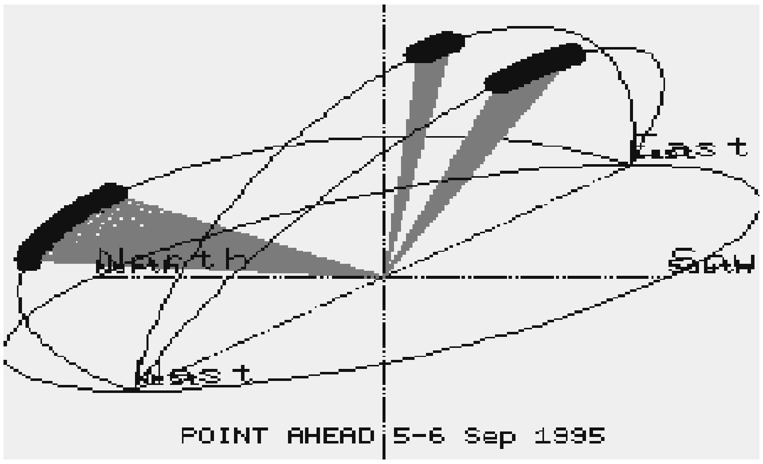

Figure 4: Point-Ahead: Comparison of simultaneous recording of seeing at La Silla measured at Zenith and at 20 degrees above northern horizon (detection of low altitude layers).

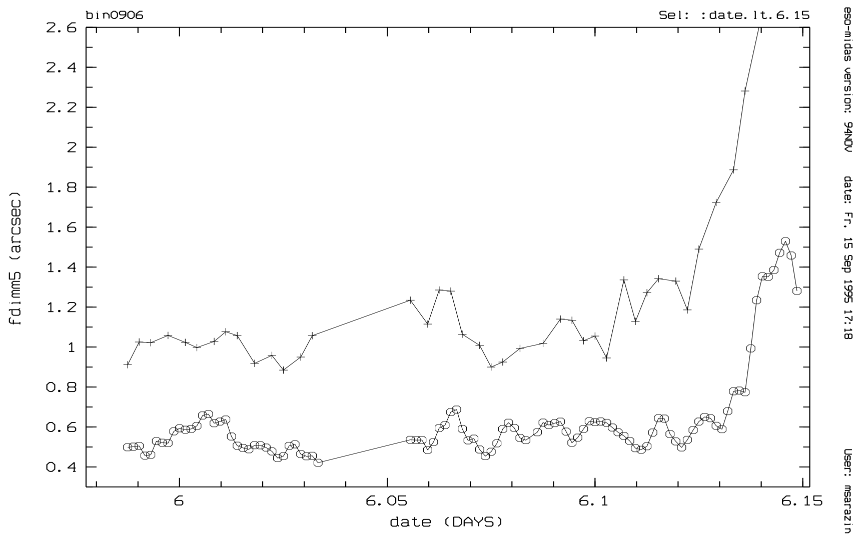

Figure 5: Point-Ahead: The near-zenith measurements have been corrected from airmass (lower curve), the near-horizon measurements (upper curve) are not corrected from airmass (approx AM=3) which produces the x2 scaling factor.

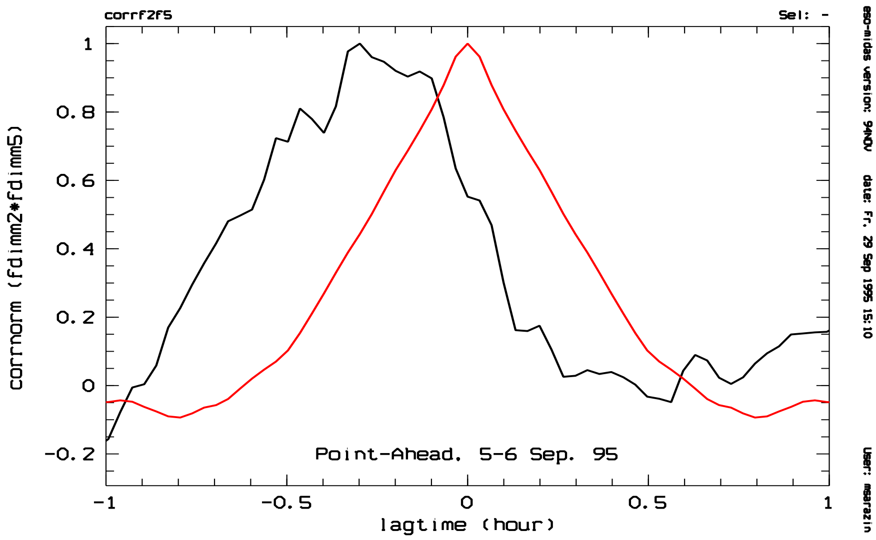

Figure 6: Point-Ahead: Intercorrelation versus Autocorrelation of the zenith seeing